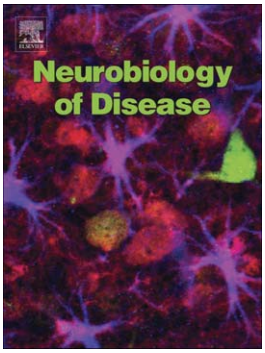

Differentiating Alzheimer Disease-Associated Aggregates with Small Molecules

Nicolette S. Honson, Ronald L. Johnson, Wenwei Huang, James Inglese, Christopher P. Austin, Jeff Kuret

PII: S0969-9961(07)00164-7
DOI: doi: 10.1016/j.nbd.2007.07.018
Reference: YNBDI 1532

To appear in: *Neurobiology of Disease*

Received date: 2 July 2007
Accepted date: 11 July 2007

Please cite this article as: Honson, Nicolette S., Johnson, Ronald L., Huang, Wenwei, Inglese, James, Austin, Christopher P., Kuret, Jeff, Differentiating Alzheimer Disease-Associated Aggregates with Small Molecules, *Neurobiology of Disease* (2007), doi: 10.1016/j.nbd.2007.07.018

Differentiating Alzheimer Disease-Associated Aggregates with Small Molecules

Nicolette S. Honson[a], Ronald L. Johnson[b], Wenwei Huang[b], James Inglese[b], Christopher P. Austin[b], and Jeff Kuret[a,*]

[a]*Center for Molecular Neurobiology, The Ohio State University, Columbus, OH 43210*
[b]*NIH Chemical Genomics Center, Rockville, MD 20850*

***Corresponding Author:**

Jeff Kuret, Ph.D.
Center for Molecular Neurobiology
1060 Carmack Rd.
Columbus, OH 43210
kuret.3@osu.edu
Tel: (614) 688-5899
Fax: (614) 292-5379

Article type: Regular article

ABSTRACT

Alzheimer disease is diagnosed postmortem by the density and spatial distribution of β-amyloid plaques and tau-bearing neurofibrillary tangles. The major protein component of each lesion adopts cross-β-sheet conformation capable of binding small molecules with submicromolar affinity. In many cases, however, Alzheimer pathology overlaps with Lewy body disease, characterized by the accumulation of a third cross-β-sheet forming protein, α-synuclein. To determine the feasibility of distinguishing tau aggregates from β-amyloid and α-synuclein aggregates with small molecule probes, a library containing 71,975 small molecules was screened for antagonists of tau-aggregate mediated changes in Thioflavin S fluorescence, followed by secondary screens to distinguish the relative affinity for each substrate protein. Results showed that >10-fold binding selectivity among substrates could be achieved, with molecules selective for tau aggregates containing at least three aromatic or rigid moieties connected by two rotatable bonds.

Key words: Alzheimer disease, tau, neurofibrillary tangle, contrast agents, diagnosis

INTRODUCTION

Alzheimer disease (AD) is the most common cause of dementia in the elderly population (Hebert et al., 2003). It is defined and definitively diagnosed by the appearance of extracellular β-amyloid (Aβ) plaques and intracellular neurofibrillary lesions in the brain (Hyman, 1997). Because AD progresses hierarchically, the density and spatial distribution of lesions also yield information on disease stage. However, all lesions are not equivalent in this regard, as total plaque density correlates poorly with cognitive decline and neurodegeneration (Braak and Braak, 1991; Terry et al., 1991). For example, substantial numbers of diffuse plaques have been found in cognitively normal elderly individuals (Hashimoto and Masliah, 1999). In contrast, neurofibrillary lesion formation correlates more closely with disease progression (Braak and Braak, 1991). These lesions consist of neurofibrillary tangles in neuronal cell bodies, neuropil threads within neuronal processes, and dystrophic neurites associated with neuritic plaques, each of which contains filamentous aggregates composed of the microtubule-associated protein tau (Buee et al., 2000). Longitudinal studies have shown that tau lesions develop according to a common spatiotemporal pattern reflecting the sequence, type and severity of cognitive decline and neuronal loss (Ghoshal et al., 2002; Royall et al., 2002). Most importantly, tau pathology appears in certain areas (such as deep temporal lobe) decades before neocortical Aβ deposition and signs of dementia can be detected (Duyckaerts and Hauw, 1997; Morsch et al., 1999), and so can serve a prognostic function. Together these data suggest that the spatial distribution and density of neuritic lesions alone can contribute to the differential diagnosis and staging of AD.

Both tau and Aβ filaments consist of parallel, in register β-sheets aligned perpendicular to the fibril axis, resulting in a cross-β-sheet structure (Petkova et al., 2006). The parallel orientation of β-sheets generates channels extending along the length of the filament (Krebs et al., 2005) to

which aromatic molecules can bind *via* π–π interactions (Gazit, 2002). Small molecules with these binding properties, including the benzothiazole aniline Pittsburgh Compound B (Klunk et al., 2004; Klunk et al., 2005), bis-styryl benzene derivatives (Kung et al., 2003), and substituted naphthalenes (Agdeppa et al., 2003), have been developed as contrast agents for use in various modalities of whole brain imaging to capture the spatial distribution of amyloid lesions *in situ* (Klunk et al., 2004). Most of these ligands bind cross-β-sheet structure common to both tau and β-amyloid bearing lesions (Berriman et al., 2003; Petkova et al., 2006), suggesting that the staging information associated with neuritic lesions will be confounded by crossreactivity with amyloid plaques. Thus, while a promising approach for following total amyloid burden, it is suboptimal as an AD diagnostic. Moreover, because α-synuclein adopts a cross-β-sheet conformation in Parkinson's disease and Lewy body disease, both of which overlap with AD in many cases (Jellinger, 2004; Kotzbauer et al., 2001), nonselective contrast agents may also detect lesions unrelated to neurofibrillary and amyloid pathology. It is likely, therefore, that contrast agents with selectivity for neurofibrillary lesions relative to Lewy bodies and Aβ plaques will have the greatest utility for staging AD and distinguishing it from other neurodegenerative diseases.

Ideally, tau-selective binding agents should interact with aggregates composed of full-length tau protein, which appear early in lesion formation and precede the formation of insoluble proteolytic products (Guillozet-Bongaarts et al., 2005). Although monomeric full-length tau proteins normally behave as random coils with limited tertiary structure (Schweers et al., 1994), they do not aggregate over experimentally tractable time periods when incubated *in vitro* under near physiological conditions of temperature, pH, ionic strength, and reducing environment (Necula and Kuret, 2004). The barrier to aggregation can be overcome by the addition of anionic

inducers such as alkyl sulfate detergents and fatty acids (Chirita et al., 2003; Wilson and Binder, 1997). Full-length tau proteins incubated in the presence of anionic surfactant inducers yield products that react with commonly used fluorescent probes for cross-β-sheet conformation such as Thioflavin S (ThS) and T (ThT) (Chirita et al., 2005). The reaction supports aggregation at low micromolar bulk tau concentrations, which facilitates screening for high affinity ligands. Although both Aβ and α-synuclein aggregate spontaneously without exogenous agents, the presence of anionic surfactant speeds aggregation rate and lowers bulk protein levels required for fibrillization (Necula et al., 2003; Wilson and Binder, 1997). As a result, it is possible to compare ligand binding to all three major AD/Lewy body disease associated protein targets under identical conditions.

To identify tau-binding agents, a ~72,000-member library of small molecules was screened using a concentration-response method termed quantitative high throughput screening (qHTS) (Inglese et al., 2006). Chosen actives were then tested in parallel assays to find selective compounds for tau, α-synuclein, and $A\beta_{1-42}$ filaments. The results show the feasibility of identifying ligands with at least an order of magnitude binding selectivity for tau relative to $A\beta_{1-42}$ and α-synuclein.

MATERIALS AND METHODS

Reagents. ThS, Type II-A mixed histones, dithiothreitol, 3,3′-Diethyl-9-methylthiacarbocyanine iodide, and arachidonic acid were purchased from Sigma-Aldrich (St Louis, MO). Octadecyl sodium sulfate (ODS) was acquired from Research Plus (Manasquan, NJ), DMSO (certified A.C.S. grade) from Fisher Scientific (Pittsburgh, PA), Thiazine red R (**1a**; Chemical Abstract Service registry number 2150-33-6) from ICN Biomedicals Inc. (Irvine, CA), **1d** from Chembridge (San Diego, CA), and HEPES from Mediatech (Herndon, VA).

Stock solutions of ODS and arachidonic acid were prepared just prior to use in 1:1 isopropanol/ddH_2O or ethanol, respectively, whereas the fluorescence reporter ThS was prepared in ddH_2O. All library compounds were prepared as 10 mM stock solutions in DMSO and stored frozen at -20ºC until used.

Recombinant His_6-htau40 and His_6-α-synuclein were prepared and stored as described previously (Carmel et al., 1996; Necula et al., 2003). Solutions of human $A\beta_{1-42}$ (American Peptide Co., Sunnyvale, CA) were prepared by established methods (Stine et al., 2003). Briefly, the peptide was resuspended in hexafluoroisopropanol (by vortexing in a glass vial) to a final concentration of 1 mM. The solvent was then completely evaporated under a slow stream of argon. The remaining residue was dissolved in DMSO to a final concentration of 2.5 mM, then sonicated for 10 min using setting 3 (model 100, Fisher Scientific).

Compound library. The 71,975 member library was collected from several sources: 1280 compounds from Sigma-Aldrich (LOPAC1280), 1120 compounds from Prestwick Chemical Inc. (Washington, DC), 280 purified natural products from TimTec (Newark, DE), three 1000-member combinatorial libraries from Pharmacopeia (Cranbury, NJ), 1106 compounds from Tocris (Ellisville, MO), 59,688 compounds from the NIH Molecular Libraries Small Molecule

Repository (San Francisco, CA), 1980 compounds from the National Cancer Institute (Bethesda, MD), and 1121 compounds from Boston University Center for Chemical Methodology and Library Development. Libraries were prepared as described (Inglese et al., 2006).

Fluorescence assays. ThS is a fluorescent probe which undergoes excitation and emission Stokes shifts upon binding neurofibrillary lesions in thin sections and tau aggregates *in vitro* (Friedhoff et al., 1998; King et al., 1999). Tau-dependent ThS fluorescence was measured as described previously (Chirita et al., 2005; King et al., 1999) with the following modifications. For qHTS, His_6-htau40 (1 μM final concentration) or mixed histones (50 nM final concentration) in reagent buffer (10 mM HEPES, pH 7.4, 100 mM NaCl, 5 mM dithiothreitol, 10 μM ThS) was dispensed (2 μL/well) into Grenier solid black 1536-well plates using a solenoid-based dispenser. Compounds (23 nL) were then transferred to the assay plate by a pin tool containing 10 nL slotted pins. Following transfer, ODS (30 μM final concentration) in reagent buffer was dispensed (2 μL/well) for a final assay volume of 4 μL /well. Following incubation (15 h at 37ºC), fluorescence (λ_{ex} = 450/8 nm; λ_{em} = 510/23 nm) was detected by an EnVision Multilabel Plate Reader (Perkin Elmer, Wellesley, MA). The screen was performed using a fully integrated Kalypsys robotic system containing one RX-130 and two RX-90 Staübli anthropomorphic robotic arms.

For determination of ThS binding affinity and secondary assays conducted in 96-well format (round bottom opaque plates, VWR, West Chester, PA), His_6-htau40, His_6-α-synuclein, or $A\beta_{1-42}$ was diluted to 5 μM in assembly buffer (10 mM HEPES, pH 7.4, 100 mM NaCl, 5 mM dithiothreitol) containing 50 μM arachidonic acid inducer. ThS probe was then added to a final concentration of 0-30 μM for ThS binding affinity determinations. Secondary assays held ThS concentrations constant at 10 μM, with library compounds selected on the basis of the qHTS

present at final concentrations of 1.52 nM to 10 μM. Each compound was tested at least twice in separate assays. Controls without protein or without compound were included on each plate. After shaking 2 min to promote mixing, plates were covered with self-adhesive aluminum foil and incubated overnight at 37ºC. Fluorescence (λ_{ex} = 440 nm; λ_{em} = 485 nm) was measured after brief shaking (10 s) in a FlexStation plate reader (Molecular Devices, Sunnyvale, CA) operated at sensitivity 10, automatic PMT.

Data analysis. qHTS data were corrected and normalized using Assay Analyzer (GeneData) as described (Inglese et al., 2006). Percent activity was calculated by normalization to the median values of the histone negative control and tau positive control present on each plate (Chirita and Kuret, 2004). For each library compound, a titration response series was generated, curve-fit, and classified as described (Inglese et al., 2006). SAR analysis was performed as described (Inglese et al., 2006).

For determination of ThS binding affinity to each substrate protein, net fluorescence was calculated by subtracting the fluorescence of the wells without protein from the fluorescence of wells containing protein. Dissociation constants (K_D) were then determined after fitting data to a rectangular hyperbola:

$$F = \frac{F_{max} x}{K_D + x} \qquad \text{(eq 1)}$$

where F represents the net ThS fluorescence at x concentration of ThS, and F_{max} is the net fluorescence at infinite ThS concentration. For secondary screens in 96-well format, net fluorescence was calculated by subtracting the fluorescence of the wells without protein from the fluorescence of wells containing both protein and compound. Percent activity was calculated by dividing net fluorescence values of treated wells with control wells containing protein but no test compound. Data were then fit to the sigmoidal function:

$$F = F_{\min} + \frac{F_{\max} - F_{\min}}{1 + 10^{(\log AC_{50} - x)n}} \qquad \text{(eq 2)}$$

where F and $F_{\max}$ are blank-adjusted ThS fluorescence in the presence and absence of inhibitor (at concentration x), respectively, $F_{\min}$ represents fluorescence at infinite ligand concentration, $\log AC_{50}$ is the log of the compound concentration producing 50% inhibition of the ThS fluorescence, and n is the Hill coefficient. Resultant AC_{50} values were converted to apparent K_i values by the Cheng-Prusoff equation (Cheng and Prusoff, 1973):

$$K_i = \frac{AC_{50}}{1 + x / K_D} \qquad \text{(eq 3)}$$

All parameters estimated by nonlinear regression are reported ± standard error of the estimate.

Fibrillization assay. Aggregation of His_6-htau40 (5 μM final concentration) in assembly buffer was induced with arachidonic acid (50 μM final concentration) in the presence or absence of selected library compounds. After incubation (18 h at 37°C) reactions were diluted 5-fold in ddH_20, and assayed by transmission electron microscopy as described previously (Necula and Kuret, 2004).

RESULTS

Initial qHTS. Thioflavin S (ThS) fluorescence was used to monitor tau conformation. ThS-reactive tau was prepared with octadecyl sulfate (ODS), an alkyl sulfate inducer of tau conformational change and aggregation (Chirita et al., 2003). Full-length tau was used as substrate because it aggregates in early stage AD and precedes the formation of aggregated truncation products (Guillozet-Bongaarts et al., 2005). Full-length tau aggregates therefore represent an early marker for AD progression. ODS was used as inducer because it efficiently drives conformational changes at low concentrations of full-length tau (low micromolar) over short time periods (≤24 h) under reducing conditions (Chirita et al., 2003). Low substrate concentrations maximize the likelihood of detecting high affinity ligands (Copeland, 2005). Mixed histones replaced tau protein in some assays to control for nonspecific alkyl-sulfate mediated effects on ThS (Chirita et al., 2005; Friedhoff et al., 1998). Histones drive micellization of anionic surfactants much like tau protein, but do not form filaments or other ThS-reactive species (Chirita and Kuret, 2004). Therefore, the final assay quantified net tau-dependent changes in ThS fluorescence.

To identify ligands capable of interfering with this signal, a 71,795-member library was screened at seven or more concentrations. The 448 plate run resulted in a mean signal to background ratio of 3.0 ± 0.2 and a mean Z' value of 0.68 ± 0.12. The concentration-response data for each compound were processed as described in Experimental Procedures, then grouped according to curve-fit and efficacy criteria (Inglese et al., 2006). Compounds with inhibitory curves having either both upper and lower asymptotes with ≥30% efficacy, or only an upper asymptote with ≥80% efficacy, were studied for structure-activity relationships. From this initial characterization, 45 compounds representing 35 active and 10 structurally-related inactive

analogs were chosen for follow-up study.

Secondary screen. To exclude nonspecific alkyl-sulfate mediated effects on ThS fluorescence, the inducer arachidonic acid replaced ODS (which was used in the initial qHTS) in a secondary screen. In addition, tau concentration was raised to 5 μM to facilitate subsequent comparison with substrates α-synuclein and $A\beta_{1-42}$. Of the 35 actives identified in the qHTS, all but eight showed similar dose-response curves and half-maximal activity concentration (AC_{50}) values in the presence of arachidonic acid (data shown below). These eight inactive compounds were eliminated from further testing, whereas compounds **1a** and **1d** were added to the library because of their established binding affinity for protein aggregates. Compound **1a** (Thiazine red R) selectively binds neurofibrillary lesions in AD tissue (Mena et al., 1995), whereas **1d** binds Aβ aggregates *in vitro* (Caprathe et al., 1999). The final test set contained 39 compounds, of which 29 showed AC_{50} < 10 μM (including nine with submicromolar AC_{50}) and 10 were inactive analogs (AC_{50} >> 10 μM).

Structures of compounds identified from the screens and characterized below, including structurally-related inactive analogs, are shown in **Fig. 1**. These were loosely grouped into six scaffold classes: benzothiazoles (**1a**, **1b**, **1c, 1d**), phenylazenes (**2a**, **2b**), quinoxaline nitriles (**3a**, **3b**, **3c**, **3d**), anilines (**4a**, **4b**, **4c**), anthraquinones (**5a**, **5b**), and indolinones (**6a**, **6b**). Concentration-effect curves for selective compounds identified from the secondary screen are shown in **Fig. 2**, with resultant AC_{50} values summarized in **Table 1**.

Identification of compounds with binding selectivity. After the primary and secondary screens identified compounds with binding affinity for tau, a selectivity screen was employed to assess their relative affinity for tau, α-synuclein, and $A\beta_{1-42}$. First, the affinity of ThS probe for each substrate was estimated from the ThS concentration dependence of fluorescent signal at constant

bulk protein concentration (5 μM). The resultant concentration effect curves were fit to retangular hyperbolas yielding apparent K_D estimates of 1.0 ± 0.1, 5.5 ± 0.7, 2.5 ± 0.4 μM for tau, α-synuclein, and $A\beta_{1-42}$, respectively (**Fig. 3**). Second, the selectivity of the test set for tau protein was determined by identical ThS-based fluorescence assays conducted in parallel with fibrillar α-synuclein and $A\beta_{1-42}$ as substrate. AC_{50} values were then converted to apparent K_i values *via* the Cheng-Prusoff equation for competitive inhibition (eq 3) using K_D values for ThS binding determined above. Differences in potency were quantified as "fold selectivity", defined as the ratio of K_i values for a given compound obtained for the lower potency substrate target divided by that of the higher potency substrate target. Thus, larger "fold selectivity" values reflected greater discrimination among the substrate proteins. Attention was focused on compounds with fold selectivities that were either statistically significant at $p < 0.05$ (for data derived from complete concentration response curves) or that were ≥10-fold in magnitude (for data derived from incomplete concentration response curves). Calculated K_i values and fold selectivities are summarized in **Table 1**. Relative selectivity is depicted graphically in **Fig. 4**.

Several compounds displayed statistically significant ($p < 0.05$) fold selectivity for tau relative to at least one other substrate. Evans blue (**2b**), and the aniline Crystal violet (**4b**) were exclusively selective for tau against both α-synuclein and $A\beta_{1-42}$ (**Table 1**, **Fig. 4**). A third compound, Thiazine red R (**1a**), was the most selective ligand in the test set, with >17-fold selectivity for tau relative to α-synuclein and was >10-fold selective against $A\beta_{1-42}$ (**Table 1, Fig. 4**). Estimates for this ligand were only approximate because concentration effect curves against non-selective substrates α-synuclein and $A\beta_{1-42}$ did not reach AC_{50} at the highest concentration tested (10 μM). Although Evans blue (**2b**) was less selective for tau than Thiazine red R (**1a**), it was ~10-fold more potent in all assays. Crystal violet (**4b**) showed only subtle

selectivity, but was among the most potent compounds tested, regardless of substrate.

In contrast to these ligands, the benzothiazole **1d,** the aniline **4a**, the anthraquinone **5a**, and the indolinone **6a** were all selective for both tau and $A\beta_{1\text{-}42}$ relative to α-synuclein (**Table 1**, **Fig. 4**). Benzothiazole **1d** was highly potent (low nanomolar K_i), and the only compound to show partial ThS-binding antagonist activity. No compounds in the test set were exclusively selective for either α-synuclein or $A\beta_{1\text{-}42}$.

Identification of high affinity ligands. Molecules which bound at least one substrate protein with submicromolar AC_{50} were identified from the test set (**Fig. 2**, **Table 1**). These included the benzothiazole **1d**, phenylazenes **2a** and **2b**, quinoxaline nitriles **3a** and **3b**, anilines **4a** and **4b**, the anthraquinone **5a**, and the indolinone **6a**. Thiazine red R (**1a**) and Adriamycin (**5b**) exhibited substoichiometric binding only for tau and $A\beta_{1\text{-}42}$, respectively, while the quinoxaline nitrile **3d** showed substoichiometric binding to all three substrate proteins (**Table 1**). Five structurally related analogs of active scaffolds did not antagonize ThS fluorescence of any substrate protein at concentrations up to 10 μM (**Table 1**). These data revealed quinoxaline nitriles to be a novel class of protein aggregate binders.

Antagonists act primarily through probe displacement. Ligand-induced decreases in ThS fluorescence could result from displacement or ThS binding or through reduction in the concentration of binding target owing to antagonism of fibrillization. To discriminate between these possibilities, tau aggregation was induced with arachidonic acid in the presence of selective compounds and analyzed by transmission electron microscopy. Typically, ~50% of tau protomer is incorporated into filaments under these conditions (Chirita et al., 2003). Seven test set compounds were assayed including three tau selective compounds (**1a**, **2b**, and **4b**) as well as the four tau and $A\beta_{1\text{-}42}$ selective compounds (**1d**, **4a**, **5a**, and **6a**). In the presence of DMSO vehicle

alone, tau aggregated to form large numbers of filaments (images not shown). However, the presence of the anilines **4a** and **4b**, as well as the indolinone **6a**, produced concentration dependant decreases in filament lengths. Fibrillization antagonist potencies were ~4-fold weaker than AC_{50} values determined by the fluorescence assay (**Fig. 5**). In contrast, levels of aggregation in the presence of the tau selective compound Thiazine red R **1a** were not statistically different from the control reaction at $p < 0.05$ (**Fig. 5**). These data confirmed that only a subset of compounds were inhibitors of tau aggregation, and suggest that the majority act as ThS displacement agents in the low concentration regime.

DISCUSSION

As expected from their shared structural organization, aggregates composed of tau, α-synuclein, and $A\beta_{1-42}$ display an overlapping continuum of small-molecule binding affinities. The general binding trends of the six scaffold classes identified in this study (**Fig. 4**) showed tau aggregates to be the most discriminating substrate tested with the strongest binding affinities, whereas α-synuclein fibrils were the least discriminating and exhibited weaker overall affinity for the compounds tested. Ligand selectivity and binding affinity for $A\beta_{1-42}$ aggregates were intermediate between those of tau and α-synuclein. This spectrum of behavior can be leveraged to identify selective binding ligands. We found that the benzothiazole **1a** and the phenylazene **2b** were exclusively selective for tau. A structural feature shared between **1a** and **2b** is the presence of at least three aromatic or rigid moieties connected by two rotatable bonds. This organization separates the rings at defined distances while allowing certain geometries that may be important for selectivity. For efficient tau binding, this geometry has been proposed to be completely planar (Wischik et al., 2004). Another commonality is the presence of a hydroxyl group ortho to an azo linker, which has been postulated to favor the hydrazone over the azo tautomer (Antonov et al., 1998). The hydrazone tautomer can form a six-membered ring *via* hydrogen bonding (the distal azene nitrogen being the hydrogen bond acceptor; **Fig. 1**). The resultant rigidity introduced by this third ring may be important for selective interaction with tau filaments. Benzothiazoles that could not form this ring or that did not have at least three rigid moieties, such as **1d,** did not bind tau filaments selectively. Similarly, compounds predicted to favor the hydrazone tautomer but that possess only two of the three aromatic or rigid units, such as **2a**, did not discriminate between tau and $A\beta_{1-42}$ filament. Perhaps the morphology of tau filaments allows for accommodation of this third ring, while its presence is less tolerated for $A\beta_{1-}$

$_{42}$ and α-synuclein fibrils. Benzothiazoles with a different arrangement of aromatic and rigid moieties, such as **1b** and **1c**, were incapable of binding any of the three substrates tested.

Recently, 2,3-di(furan-2yl)-quinoxalines were identified as tau fibrillization inhbitors *via* a sedimentation assay and subsequent EM analysis (Crowe et al., 2007). We found the quinoxaline containing nitrile derivatives **3a**, **3b**, and **3d** to represent a novel class of filament binding molecules, which bind all three protein substrates substoichiometrically with respect to bulk protein concentration. The quinoxaline nitrile analog **3c** was inactive possibly due to a stereo-electronic effect. Here, an amide replaced the ester seen in **3a**, **3b**, and **3d**. The nitrogen from this amide allows for better electron back donation due to increased orbital overlap with the amide carbonyl. This results in reduced flexibility and a possible increased steric effect due to the presence of the bulky phenyl, which subsequently may prevent **3c** from accessing fibril channels. A similar steric effect was observed with anilines **4a**, **4b**, and **4c**, although interpretation of this series may be complicated by the tau aggregation antagonist activities of **4a** and **4b**. Crystal violet (**4b**) interacted with high affinity regardless of substrate whereas analog **4c** was inactive, again perhaps owing to steric effects. Differences in symmetry could also contribute to differences in potency. For example both **4a** and **4b** possess pseudo C_3 symmetry (assuming **4a** is capable of tautomerization under assay conditions), and so their effective concentrations could be significantly higher than that of **4c** if binding were mediated predominantly by only a portion of each molecule. Crystal violet (**4b**) was also found to be subtly selective for tau filaments, suggesting the bulky dimethylamino groups may be less tolerated by α-synuclein and $A\beta_{1\text{-}42}$ aggregates.

Comparison with previous studies. Three candidate compounds, including one benzimidazole derivative (BF-126) and two quinoline derivatives (BF-158 and BF-170), are selective for tau

over $A\beta_{1-42}$ aggregates *in vitro* (Okamura et al., 2005). Although only 2-3-fold selectivity was demonstrated, tissue staining patterns strongly favored neurofibrillary lesions over Aβ plaques in AD hippocampal brain sections (Okamura et al., 2005). These data suggest that compounds exhibiting even subtle selectivity may have utility for contrast agent development. The observations may stem from the higher bulk tau levels (~150-300 pmol/mg wet tissue; (Khatoon et al., 1992)) relative to Aβ peptide concentrations (~9 pmol/mg wet tissue; (Jellinger, 2004; Wang et al., 1999)) in late stage AD frontal and temporal cortices. Alternatively, selective staining could arise from differences in binding stoichiometry. In the case of Aβ filaments, multiple partially overlapping binding sites with differing binding affinities have been demonstrated along the length of the fibril (Lockhart et al., 2005). These differ in density from 1:300 to 1:4 ligand:Aβ molar stoichiometry (Lockhart et al., 2005). The demonstration of partial antagonism of ThS-tau interaction by high affinity ligand **1d** suggests that tau aggregates may also contain multiple binding sites, with **1d** binding to only a subset of those labeled by ThS (**Fig. 2B**). Nonetheless, it is also possible that the selective lesion staining observed in tissue resulted from binding kinetics, since ligands were presented to both neurofibrillary and Aβ lesions at saturating concentrations for a time (10 min) which may be inadequate for reaching equilibrium.

Anthraquinones including Daunorubicin (a structural analog of **5a**) and Adriamycin (presented in this study as **5b**) have previously been explored as inhibitors of tau fibrillization under non-reducing conditions (Pickhardt et al., 2005). While both compounds were active in the tau ThS displacement assay, no antagonistic effects were observed under the fibrillization conditions used here for the tau and $A\beta_{1-42}$ selective compound **5a**. Tau concentration, redox conditions, and incubation times may be the major variables contributing to this discrepancy.

Finally, the indolinone **6a** was an effective binder of all filamentous substrates tested and antagonized tau fibrillization while **6b**, which contains a bulky 1, 3, 5-methoxy tri-substituted aromatic ring situated closer to the indolinone ring system, did not bind any aggregates tested. Structurally related hydroxyindoles have previously been identified as $A\beta_{1-40}$ and $A\beta_{1-42}$ fibrillization inhibitors (Cohen et al., 2006).

Future challenges. The search for selective binding agents is further complicated by two factors. First, different filament morphologies in disease may reflect polymorphisms at the protofilament level (Petkova et al., 2005). For example, the degree of stagger (defined as the displacement of β-sheets along the long fibril axis (Petkova et al., 2006)) may result in changes in channel dimension. This may restrict ligand access to certain morphologies. Second, the existence of multiple tau isoforms may complicate detection of mixed tau aggregates. For example, high affinity binding sites on human $A\beta_{1-42}$ filaments are disrupted in filaments made from mouse/human $A\beta_{1-42}$ mixtures (Klunk et al., 2005; Ye et al., 2006). Similar microheterogeneity may affect high-affinity ligand binding to tau filaments composed of isoform mixtures.

In summary, parallel screening of the three major protein aggregates found in AD and Lewy body disease brain revealed the feasibility of selectively binding tau aggregates relative to aggregates composed of α-synuclein or $A\beta_{1-42}$. Structural analysis of the screened compounds suggested that a specific arrangement of aromatic or rigid moieties may impart tau aggregate binding selectivity. Selective compounds may serve as starting points for the synthesis of chemical analogs that, when appropriately labeled, could serve as premortem contrast agents capable of distinguishing the early stages of neurodegenerative diseases through whole brain imaging methods.

ACKNOWLEDGMENTS

We thank L. Crissman for assisting in the production of tau and α-synuclein, R. Batra for help with the transmission electron microscopy, S. Michael and C. Klumpp for assistance with automated screening, and A. Jadhav for the informatics analysis. This research was supported by grants from the National Institutes of Health (AG14452 and MH077621) and the Alzheimer Association (to J.K.), the Molecular Libraries Initiative of the NIH Roadmap for Medical Research, and the Intramural Research Program of the National Human Genome Research Institute. Data for the qHTS were deposited in Pubchem (ID 596).

REFERENCES

Agdeppa, E. D., et al., 2003. 2-Dialkylamino-6-acylmalononitrile substituted naphthalenes (DDNP analogs): novel diagnostic and therapeutic tools in Alzheimer's disease. Mol. Imaging Biol. 5**,** 404-417.

Antonov, L., et al., 1998. Theoretical investigations on the tautomerism of 1-phenylazo-4-naphthol and its isomers. Dyes Pigment. 38**,** 157-164.

Berriman, J., et al., 2003. Tau filaments from human brain and from in vitro assembly of recombinant protein show cross-beta structure. Proc. Natl. Acad. Sci. U.S.A. 100**,** 9034-9038.

Braak, H., Braak, E., 1991. Neuropathological stageing of Alzheimer-related changes. Acta Neuropathol. (Berl.). 82**,** 239-259.

Buee, L., et al., 2000. Tau protein isoforms, phosphorylation and role in neurodegenerative disorders. Brain Res. Brain Res. Rev. 33**,** 95-130.

Caprathe, B. W., et al., 1999. Method of imaging amyloid deposits. U.S. Patent 6,001,331.

Carmel, G., et al., 1996. The structural basis of monoclonal antibody Alz50's selectivity for Alzheimer's disease pathology. J. Biol. Chem. 271**,** 32789-32795.

Cheng, Y., Prusoff, W. H., 1973. Relationship between the inhibition constant (K_I) and the concentration of inhibitor which causes 50 per cent inhibition (I_{50}) of an enzymatic reaction. Biochem. Pharmacol. 22**,** 3099-3108.

Chirita, C. N., et al., 2005. Triggers of full-length tau aggregation: a role for partially folded intermediates. Biochemistry. 44**,** 5862-5872.

Chirita, C. N., Kuret, J., 2004. Evidence for an intermediate in tau filament formation. Biochemistry. 43**,** 1704-1714.

Chirita, C. N., et al., 2003. Anionic micelles and vesicles induce tau fibrillization in vitro. J. Biol. Chem. 278**,** 25644-25650.

Cohen, T., et al., 2006. Inhibition of amyloid fibril formation and cytotoxicity by hydroxyindole derivatives. Biochemistry. 45**,** 4727-35.

Conway, K. A., et al., 2001. Kinetic stabilization of the alpha-synuclein protofibril by a dopamine-alpha-synuclein adduct. Science. 294**,** 1346-9.

Copeland, R. A., 2005. Evaluation of enzyme inhibitors in drug discovery : a guide for medicinal chemists and pharmacologists. Wiley, Hoboken, N.J.

Crowe, A., et al., 2007. High throughput screening for small molecule inhibitors of heparin-induced tau fibril formation. Biochem. Biophys. Res. Comm. 358**,** 1-6.

Duyckaerts, C., Hauw, J. J., 1997. Prevalence, incidence and duration of Braak's stages in the general population: can we know? Neurobiol. Aging. 18**,** 362-369.

Friedhoff, P., et al., 1998. Rapid assembly of Alzheimer-like paired helical filaments from microtubule-associated protein tau monitored by fluorescence in solution. Biochemistry. 37**,** 10223-10230.

Gazit, E., 2002. A possible role for pi-stacking in the self-assembly of amyloid fibrils. FASEB J. 16**,** 77-83.

Ghoshal, N., et al., 2002. Tau conformational changes correspond to impairments of episodic memory in mild cognitive impairment and Alzheimer's disease. Exp. Neurol. 177**,** 475-493.

Guillozet-Bongaarts, A. L., et al., 2005. Tau truncation during neurofibrillary tangle evolution in Alzheimer's disease. Neurobiol. Aging. 26**,** 1015-1022.

Hashimoto, M., Masliah, E., 1999. Alpha-synuclein in Lewy body disease and Alzheimer's disease. Brain Pathol. 9**,** 707-720.

Hebert, L. E., et al., 2003. Alzheimer disease in the US population: prevalence estimates using the 2000 census. Arch. Neurol. 60**,** 1119-1122.

Hyman, B. T., 1997. The neuropathological diagnosis of Alzheimer's disease: clinical-pathological studies. Neurobiol. Aging. 18**,** S27-32.

Inglese, J., et al., 2006. Quantitative high-throughput screening: a titration-based approach that efficiently identifies biological activities in large chemical libraries. Proc. Natl. Acad. Sci. U.S.A. 103**,** 11473-11478.

Jellinger, K. A., 2004. Lewy body-related alpha-synucleinopathy in the aged human brain. J. Neural. Transm. 111**,** 1219-1235.

Khatoon, S., et al., 1992. Brain levels of microtubule-associated protein tau are elevated in Alzheimer's disease: a radioimmuno-slot-blot assay for nanograms of the protein. J. Neurochem. 59**,** 750-753.

King, M. E., et al., 1999. Ligand-dependent tau filament formation: implications for Alzheimer's disease progression. Biochemistry. 38**,** 14851-14859.

Klunk, W. E., et al., 2004. Imaging brain amyloid in Alzheimer's disease with Pittsburgh Compound-B. Ann. Neurol. 55**,** 306-319.

Klunk, W. E., et al., 2005. Binding of the positron emission tomography tracer Pittsburgh compound-B reflects the amount of amyloid-beta in Alzheimer's disease brain but not in transgenic mouse brain. J. Neurosci. 25**,** 10598-10606.

Kotzbauer, P. T., et al., 2001. Lewy body pathology in Alzheimer's disease. J Mol Neurosci. 17**,** 225-32.

Krebs, M. R., et al., 2005. The binding of thioflavin-T to amyloid fibrils: localisation and implications. J. Struct. Biol. 149**,** 30-37.

Kung, M. P., et al., 2003. Detection of amyloid plaques by radioligands for Aβ40 and Aβ42: potential imaging agents in Alzheimer's patients. J. Mol. Neurosci. 20**,** 15-24.

Lockhart, A., et al., 2005. Evidence for the presence of three distinct binding sites for the thioflavin T class of Alzheimer's disease PET imaging agents on beta-amyloid peptide fibrils. J. Biol. Chem. 280**,** 7677-7684.

Mena, R., et al., 1995. Monitoring pathological assembly of tau and beta-amyloid proteins in Alzheimer's disease. Acta Neuropathol. (Berl.). 89**,** 50-56.

Morsch, R., et al., 1999. Neurons may live for decades with neurofibrillary tangles. J. Neuropathol. Exp. Neurol. 58**,** 188-197.

Necula, M., et al., 2003. Rapid anionic micelle-mediated α-synuclein fibrillization in vitro. J. Biol. Chem. 278**,** 46674-46680.

Necula, M., Kuret, J., 2004. Electron microscopy as a quantitative method for investigating tau fibrillization. Anal. Biochem. 329**,** 238-246.

Okamura, N., et al., 2005. Quinoline and benzimidazole derivatives: candidate probes for in vivo imaging of tau pathology in Alzheimer's disease. J. Neurosci. 25**,** 10857-10862.

Petkova, A. T., et al., 2005. Self-propagating, molecular-level polymorphism in Alzheimer's beta-amyloid fibrils. Science. 307**,** 262-5.

Petkova, A. T., et al., 2006. Experimental constraints on quaternary structure in Alzheimer's beta-amyloid fibrils. Biochemistry. 45**,** 498-512.

Pickhardt, M., et al., 2005. Anthraquinones inhibit tau aggregation and dissolve alzheimer paired helical filaments in vitro and in cells. J. Biol. Chem. 280**,** 3628-3635.

Royall, D. R., et al., 2002. Pathological determinants of the transition to clinical dementia in Alzheimer's disease. Exp. Aging Res. 28**,** 143-162.

Schweers, O., et al., 1994. Structural studies of tau protein and Alzheimer paired helical filaments show no evidence for beta-structure. J. Biol. Chem. 269**,** 24290-24297.

Stine, W. B., Jr., et al., 2003. In vitro characterization of conditions for amyloid-beta peptide oligomerization and fibrillogenesis. J. Biol. Chem. 278**,** 11612-11622.

Terry, R. D., et al., 1991. Physical basis of cognitive alterations in Alzheimer's disease: synapse loss is the major correlate of cognitive impairment. Ann. Neurol. 30**,** 572-580.

Wang, J., et al., 1999. The levels of soluble versus insoluble brain Abeta distinguish Alzheimer's disease from normal and pathologic aging. Exp. Neurol. 158**,** 328-337.

Wilson, D. M., Binder, L. I., 1997. Free fatty acids stimulate the polymerization of tau and amyloid beta peptides. In vitro evidence for a common effector of pathogenesis in Alzheimer's disease. Am. J. Pathol. 150**,** 2181-2195.

Wischik, C. M., et al., 2004. Neurofibrillary labels. U.S. Patent Application 0213736 A1.

Ye, L., et al., 2006. Characterisation of the binding of amyloid imaging tracers to rodent Abeta fibrils and rodent-human Abeta co-polymers. Biochem. Biophys. Res. Comm. 347**,** 669-677.

Zhu, M., et al., 2004. The flavonoid baicalein inhibits fibrillation of α-synuclein and disaggregates existing fibrils. J. Biol. Chem. 279**,** 26846-26857.

FIGURE LEGENDS

Figure 1. Structures of selected actives from the qHTS and follow up testing. NCGC compound IDs and/or common names are as follows: **1a** Thiazine red R (hydrazone tautomer), **1b** NCGC00047883-01, **1c** NCGC00048966-01, **1d**, **2a** NCGC00014816-01 (azo tautomer), **2b** Evans blue NCGC00024822-01 (azo tautomer), **3a** NCGC00070646-01, **3b** NCGC00066166-01, **3c** NCGC00072862-01, **3d** NCGC00065256-01, **4a** NCGC00013110-01, **4b** Crystal violet AB07944787-01, **4c** NCGC00013120-01, **5a** NCGC00014611-01, **5b** Adriamycin NCGC00014693-01, **6a** NCGC00025170-01, **6b** NCGC00015546-01. Compounds highlighted in grey indicate inactive structural analogs identified from both the qHTS and the selectivity screen.

Figure 2. Representative concentration effect curves for selected compounds. Five μM tau (●, solid line), α-synuclein (○, dashed line), or $A\beta_{1\text{-}42}$ (▲, dashed/dotted line) was incubated (37°C for 18 h) with arachidonic acid inducer (50 μM) in the presence of 10 μM ThS reporter and varying concentrations of compounds identified by qHTS, then subjected to fluorescence spectroscopy (λ_{ex} = 440 nm; λ_{em} = 485 nm). Each point represents the mean of two or more determinations (expressed as % fluorescence in presence of DMSO vehicle alone) whereas the lines reflect best fit of data points to equation 2. Error bars correspond to S.D. Titration response curves are shown for the following selective compounds: (**A**) Thiazine red R (**1a**) and the inactive (AC_{50} > 10 μM) Thiazine red R homolog **1b** (data shown only for tau; Δ, dotted line). (**B**) the benzothiazole **1d**, (**C**) Evans blue (**2b**), (**D**) the aniline **4a** and inactive (AC_{50} > 10 μM) analog **4c** (data shown only for $A\beta_{1\text{-}42}$; Δ, dotted line), (**E**) Crystal violet (**4b**), (**F**) the

anthraquinone **5a**, and (**G**) the indolinone **6a** and inactive (AC_{50} > 10 μM) analog **6b** (data shown only for tau; Δ, dotted line).

Figure 3. **Comparison of ThS binding affinities for each substrate protein**. ThS-based fluorescence assays were conducted in parallel with tau (●), α-synuclein (○), or $A\beta_{1-42}$ (■) as substrate. (**A**) Tau, α-synuclein, and $A\beta_{1-42}$ (each at 5 μM) were incubated (37°C for 18 h) with arachidonic acid inducer (50 μM) in the presence of 0-30 μM ThS reporter, then subjected to fluorescence spectroscopy (λ_{ex} = 440 nm; λ_{em} = 485 nm). Each point represents the mean of duplicate determinations (expressed as net fluorescence), whereas the lines reflect best fit of data points to equation 1. (**B**) Bar graph of the relative affinity of ThS for each substrate as estimated from the fitted curves in (**A**). Error bars represent the standard error of the estimate determined from fit of data points to equation 1.

Figure 4. Identification of selective binders of tau, α-synuclein, and $A\beta_{1-42}$. Molecules shown in **Fig. 1** and their associated K_i values (from **Table 1**) are depicted for tau (red), $A\beta_{1-42}$ (green), and α-synuclein (blue). The distance from the origin of the plot corresponds to the magnitude of the K_i value. Compounds selective for tau or $A\beta_{1-42}$ are marked with a red circle or a green triangle, respectively. Strongest selectivity for tau was obtained from scaffolds **1** and **2**.

Figure 5. Identification of tau aggregation antagonists. Tau (5 μM) was incubated (37°C for 18 h) with arachidonic acid inducer (50 μM) in the presence of varying concentrations of selective compounds Thiazine red R (**1a**), the aniline **4a**, Crystal violet (**4b**), and the indolinone **6a**. Each compound was tested at AC_{50} and four times the AC_{50} values as determined by the fluorescence assay, and then examined for tau fibrillization by electron microscopy. The lowest concentrations (black bars) of **1a**, **4a**, **4b**, and **6a** were 2.1 μM, 1.6 μM, 0.18 μM, and 1.0 μM, respectively. Highest concentrations (white bars) of **1a**, **4a**, **4b**, and **6a** were 8.4 μM, 6.4 μM,

0.72 μM, and 4.0 μM, respectively. Filament length (Γ_f) is reported as the percent filament length observed in the presence of DMSO vehicle alone (labeled as C, hatched bar), which is defined as 100%. Error bars indicate S.D. Statistical significance of differences in total filament length was assessed by Student's *t* test (*, $p < 0.05$).

Table 1: Compounds exhibiting selectivity and submicromolar binding affinity.

Cpd	tau		α-synuclein		$A\beta_{1-42}$		Fold Selectivity		
	AC_{50} (μM)	K_i (nM)	AC_{50} (μM)	K_i (nM)	AC_{50} (μM)	K_i (nM)	tau/ α-syn.	tau/ $A\beta_{1-42}$	$A\beta_{1-42}$/ α-syn.
1a	**2.1 ± 0.6**	**200 ± 65**	>10	>3500	>10	>2000	>17	>10	n/a
1b	>10	>940	>10	>3500	>10	>2000	n/a	n/a	n/a
1c	>10	>940	>10	>3500	>10	>2000	n/a	n/a	n/a
1d	**0.083 ± 0.004**	**7.8 ± 1.0**	>10	>3500	**0.067 ± 0.006**	**13 ± 2**	>440	1.7 ± 0.4	>260
2a	0.78 ± 0.25	74 ± 26	2.6 ± 1.5	930 ± 520	1.0 ± 0.54	200 ± 110	13 ± 8.3	2.8 ± 1.8	4.5 ± 3.5
2b	**0.19 ± 0.03**	**18 ± 3**	0.75 ± 0.08	260 ± 35	0.90 ± 0.28	180 ± 59	15 ± 3**	10 ± 4*	1.5 ± 0.5
3a	2.8 ± 0.7	260 ± 77	1.7 ± 0.3	580 ± 120	0.76 ± 0.28	150 ± 59	2.2 ± 0.8	0.6 ± 0.3	3.9 ± 1.7
3b	4.0 ± 2.3	379 ± 220	1.2 ± 0.4	440 ± 160	0.96 ± 0.15	190 ± 39	1.2 ± 0.8	0.5 ± 0.3	2.3 ± 1.0
3c	>10	>940	>10	>3500	>10	>2000	n/a	n/a	n/a
3d	2.7 ± 1.2	260 ± 110	1.8 ± 0.5	620 ± 180	3.6 ± 1.4	720 ± 290	2.4 ± 1.3	2.8 ± 1.7	0.9 ± 0.4
4a	**1.6 ± 0.3**	**150 ± 35**	2.0 ± 0.4	700 ± 160	**0.56 ± 0.09**	**110 ± 23**	4.6 ± 1.5*	0.7 ± 0.2	6.4 ± 2.0**
4b	**0.18 ± 0.01**	**17 ± 2**	0.15 ± 0.02	53 ± 8	0.15 ± 0.01	29 ± 4	3.1 ± 0.6**	1.7 ± 0.3*	1.8 ± 0.4
4c	>10	>940	>10	>3500	>10	>2000	n/a	n/a	n/a
5a	**2.1 ± 0.2**	**190 ± 30**	2.1 ± 0.3	750 ± 120	**0.55 ± 0.10**	**110 ± 24**	3.9 ± 0.9**	0.6 ± 0.2	6.9 ± 1.9**
5b	9.6 ± 7.6	910 ± 730	>10	>3500	1.6 ± 0.8	320 ± 160	>3	0.4 ± 0.3	>10
6a	**1.0 ± 0.1**	**95 ± 17**	1.4 ± 0.3	490 ± 120	**0.72 ± 0.07**	**140 ± 23**	5.1 ± 1.6*	1.5 ± 0.4	3.4 ± 1.0*
6b	>10	>940	>10	>3500	>10	>2000	n/a	n/a	n/a

Underlined values indicate compounds with AC_{50} values <1.0 μM. Values highlighted in bold indicate compounds selective for either tau or $A\beta_{1-42}$ relative to α-synuclein. Statistical significance of fold selectivity was assessed by comparison of K_i values by Student's *t* test (**, $p < 0.01$; *, $p < 0.05$). All errors = SEE.

1a

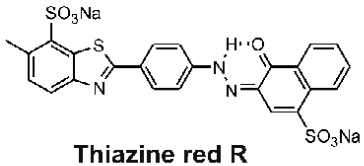

Thiazine red R

1b

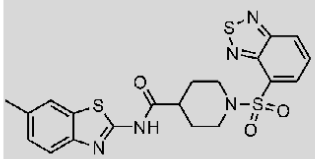

1c

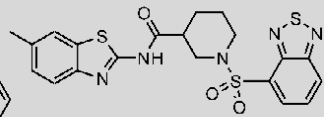

1d

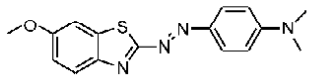

2a

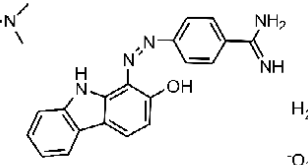

2b

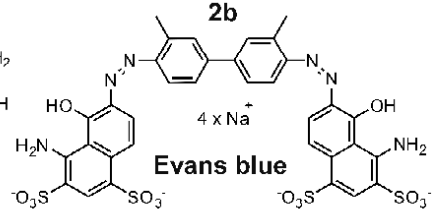

Evans blue

3a

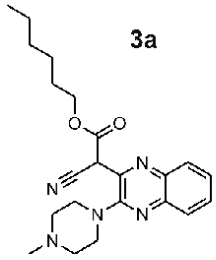

3b

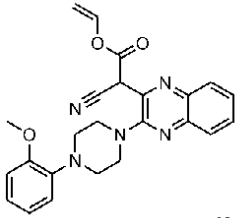

3c

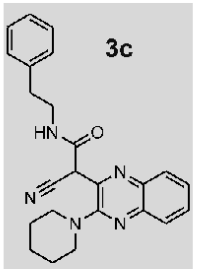

3d

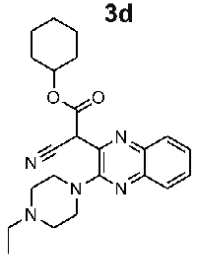

4a

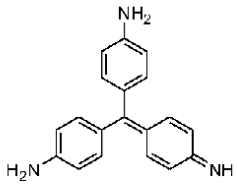

4b

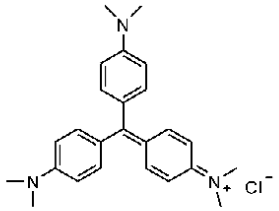

Crystal violet

4c

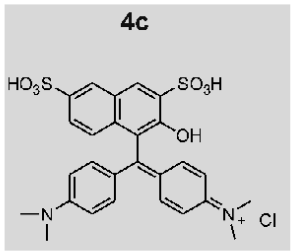

5a

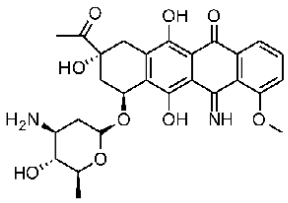

5b

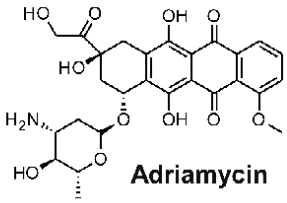

Adriamycin

6a

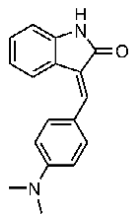

6b